

Earth and Space Science



RESEARCH ARTICLE

10.1029/2021EA002185

Key Points:

- Mean monsoon and low-pressure systems (LPS) weaken in response to the Arctic and Antarctic sea ice melt in climate model simulations
- The LPS genesis declines by 22% in response to a decline of 78% (24%) in sea ice concentrations over the Arctic (Antarctic) in the June–September season
- The decline in LPS genesis is linked to changes in low-level vorticity and vertical shear

Supporting Information:

Supporting Information may be found in the online version of this article.

Correspondence to:

S. Sandeep,
sandeep.sukumaran@cas.iitd.ac.in

Citation:

Chandra, V., Sandeep, S., Suhas, E., & Subramanian, A. C. (2022). Weakening of Indian summer monsoon synoptic activity in response to polar sea ice melt induced by albedo reduction in a climate model. *Earth and Space Science*, 9, e2021EA002185. <https://doi.org/10.1029/2021EA002185>

Received 14 DEC 2021

Accepted 25 JUL 2022





Author Contributions:

Conceptualization: S. Sandeep
Data curation: Varunesh Chandra
Formal analysis: Varunesh Chandra, S. Sandeep, E. Suhas, Aneesh C. Subramanian
Funding acquisition: S. Sandeep
Investigation: Varunesh Chandra, S. Sandeep, E. Suhas, Aneesh C. Subramanian

© 2022. The Authors. Earth and Space Science published by Wiley Periodicals LLC on behalf of American Geophysical Union.

This is an open access article under the terms of the [Creative Commons Attribution-NonCommercial-NoDerivs License](https://creativecommons.org/licenses/by/4.0/), which permits use and distribution in any medium, provided the original work is properly cited, the use is non-commercial and no modifications or adaptations are made.

Weakening of Indian Summer Monsoon Synoptic Activity in Response to Polar Sea Ice Melt Induced by Albedo Reduction in a Climate Model

Varunesh Chandra¹ , S. Sandeep¹ , E. Suhas² , and Aneesh C. Subramanian³ 

¹Centre for Atmospheric Sciences, Indian Institute of Technology Delhi, New Delhi, India, ²Earth and Climate Sciences, Indian Institute of Science Education and Research Pune, Pune, India, ³Department of Atmospheric and Oceanic Sciences, University of Colorado Boulder, Boulder, CO, USA

Abstract The effect of polar sea ice melt on low latitude climate is little known. To understand the response of the Indian summer monsoon (ISM) synoptic activity to the sea ice melt, we have run a suite of coupled and uncoupled climate model simulations. In one set of simulations, the albedo of sea ice is reduced so that it would melt due to increased absorption of solar radiation. The coupled model simulation with a reduced sea ice albedo resulted in an almost complete melting of the sea ice in summer in both hemispheres. A high-resolution (50 km) atmospheric general circulation model (AGCM) is forced with the climatological annual cycles of sea surface temperature (SST) and sea ice concentrations (SIC) from the coupled model outputs to better resolve synoptic scale variability. In the high-resolution AGCM simulations forced with SST and SIC from the sea ice melt experiments, the ISM circulation weakened substantially, and the monsoon low-pressure systems (LPS) activity experienced an overall decline of 23%, with a widespread weakening in the south and a moderate strengthening over the north, in response to a decline of 78% (24%) in SIC over the Arctic (Antarctic) in the June–September season. The changes in the LPS activity in response to polar sea ice melt are found to be mostly driven by the changes in low-level absolute vorticity and vertical shear over the Bay of Bengal.

Plain Language Summary The sea ice is melting rapidly in a warming climate, which can have feedback effects on the climate system. However, the impact of sea ice melt on low latitude climate is not adequately understood. The Indian summer monsoon (ISM), known as the lifeline of South Asia, is essential to the water security of more than 1.5 billion people. We examined the response of the ISM to the polar sea ice melt using a suite of global climate model experiments. Our simulations show that the monsoon circulation and rainfall weaken substantially due to the sea ice melt. Further, the number of propagating precipitating vortices embedded in the monsoon circulation declined by about 22% in the sea ice melt experiments. Our results suggest that the Arctic and Antarctic sea ice melt could have severe implications for the water security of South Asia.

1. Introduction

The Arctic sea ice has been melting rapidly in recent decades in response to a warming climate (Lindsay & Zhang, 2005; Overland & Wang, 2013). The climate model projections indicate that the Arctic would experience an ice-free summer by the second half of the 21st century at the current rate of global warming (Overland & Wang, 2013). The Antarctic sea ice variability is more complex compared to that of the Arctic, with a slight increasing trend in the sea ice extent for the first three decades of the satellite era and a decreasing trend in recent years that is faster than the rate of Arctic sea ice melt (Parkinson, 2019). Further, the Antarctic summer sea ice is also projected to vanish by the end of the 21st century under strong warming scenarios (Roach et al., 2020). The polar sea ice melt can have far-reaching effects on the global climate system through surface energy imbalance and the response of ocean dynamics (Screen & Simmonds, 2010; Serreze & Barry, 2011). Due to the thermal inertia of the oceans, the effect of sea ice melt can persist for multiple seasons (Francis et al., 2009). Experiments using atmospheric general circulation models (AGCM) have shown that Arctic sea ice depletion explains most of the seasonal patterns of high-latitude climate response to enhanced greenhouse gas (GHG) warming (Deser et al., 2010).

The effects of sea ice melt and the Arctic amplification on midlatitude climate are evident through the changes in storm tracks, jetstream, and the Rossby wave activity (Francis & Vavrus, 2012; Rinke et al., 2017). These changes

Methodology: Varunesh Chandra, S. Sandeep, E. Suhas, Aneesh C. Subramanian
Project Administration: S. Sandeep
Resources: S. Sandeep
Software: Varunesh Chandra
Supervision: S. Sandeep
Validation: Varunesh Chandra
Visualization: Varunesh Chandra
Writing – original draft: Varunesh Chandra, S. Sandeep
Writing – review & editing: Varunesh Chandra, S. Sandeep, E. Suhas, Aneesh C. Subramanian

cause an increased frequency of extreme weather events, such as floods, heatwaves, and severe cyclonic storms in the middle- and high-latitude regions (Budikova, 2009; Cohen et al., 2014, 2020). The impact of sea ice melt on low latitude weather has only recently received attention from the research community. One possible channel for the changes in the Arctic to influence the tropics is through the response of oceanic heat transport (Tomas et al., 2016). It is well-known that the Atlantic meridional overturning cell, which plays a crucial role in oceanic heat transport, will weaken in response to the Arctic sea ice melt (Liu & Fedorov, 2019; Sevellec et al., 2017). The atmospheric thickness response to the Arctic amplification and subsequent changes in the equatorward Rossby wave propagation can be another channel for Arctic to tropics teleconnection (Francis & Vavrus, 2012). However, the low latitude response to the Arctic sea ice melt was not evident in tropical extreme weather events (Barnes et al., 2014; Wallace et al., 2014).

Quantifying the response of sea ice melt to the climate system using observational analysis is difficult due to the presence of multiple variability with different spatio temporal scales in the observed data. The climate models, although not perfect, are useful tools in understanding the response of the sea ice melt to the climate system (Smith et al., 2019). In climate model simulations, in the absence of ocean dynamics, the effect of Arctic sea ice melt is largely confined to regions poleward of 30°N while the addition of ocean dynamics resulted in an equatorward shift of the inter-tropical convergence zone (ITCZ) (Deser et al., 2015; Liu & Fedorov, 2019). When only the thermodynamic coupling is retained by suppressing dynamic coupling, the ITCZ and Hadley cell shifted poleward in response to the Arctic sea ice melt (Tomas et al., 2016). The changes in the mean position of ITCZ can affect the tropical cyclone (TC) genesis (Berry & Reeder, 2014; Molinari & Vollaro, 2013). Aquaplanet simulations suggest that a poleward shift in the ITCZ would result in an increased frequency of TC-like synoptic scale weather systems (Ballinger et al., 2015). Deng et al. (2018) argued that the variability in the Arctic sea ice might influence the mid-Pacific trough, which in turn can affect the TC genesis over the northwest Pacific. The response of ocean dynamics to the sea ice melt can induce a global oceanic response (Deser et al., 2010; Liu & Fedorov, 2019). Such an oceanic response can have far-reaching effects on Earth's climate system, including tropical cyclones and monsoons. However, the effect of polar sea ice melt on monsoons and tropical cyclones is poorly understood. Hence, we perform a coupled climate model simulation followed by an uncoupled high-resolution AGCM simulation forced with sea surface temperature (SST) and sea ice concentrations (SIC) from coupled model outputs to understand the effect of polar sea ice melt on monsoon synoptic systems.

The remote influences of extratropical variability on the Indian summer monsoon (ISM) have long been known (Buermann et al., 2005; Khandekar, 1991). The operational seasonal forecasts over India used extratropical parameters to predict the forthcoming summer monsoon (Rajeevan, 2002). Recently, a link between the Atlantic SST and ISM is also emerging (Pottapinjara et al., 2014; Sabeerali et al., 2019, 2021). The Atlantic meridional overturning circulation is slowing down in response to the Arctic sea ice melt (Smeed et al., 2014) that may add more complexity to the teleconnection between the Atlantic SST and ISM. Earlier studies suggested a possible teleconnection between the Arctic and Antarctic sea ice variability and the Asian summer monsoon on intraseasonal and interannual scales (Chatterjee et al., 2021; Guo et al., 2014; Prabhu et al., 2012, 2021). The influence of tropical variability on the Arctic was also reported (Krishnamurti et al., 2015; Nuncio et al., 2020). However, those studies relied on the statistical analysis of the observed data, which may not be sufficient to understand the underlying mechanisms. A sensitivity experiment using a coupled climate model is better suited to understand teleconnection mechanisms in detail.

The monsoon synoptic activity over India is known to be influenced by remote forcing from the Pacific and Atlantic (Meera et al., 2019; Pottapinjara et al., 2014; Srujan et al., 2021, 2022). Further, in future warming simulations, the synoptic storms are found to be weakening (Dong et al., 2020; Rastogi et al., 2018; Sandeep et al., 2018). In idealized experiments, Sørland et al. (2016) found that the rainfall associated with the monsoon LPS scales at a Clausius-Clapeyron rate in response to the imposed warming. The response of monsoon synoptic activity to the sea ice melt is not known. In this paper, we explore the possible changes in the ISM synoptic activity due to the polar sea ice melt.

One of the reasons for the lack of understanding of the effect of sea ice melt on the genesis of high impact tropical weather systems is that the coarse-resolution simulations using coupled models do not adequately resolve TCs and monsoon low-pressure systems (LPS). One way to overcome this issue is to run high-resolution AGCM simulations forced with SST and SIC from coupled model experiments (Murakami et al., 2011; Sabin et al., 2013; Sandeep et al., 2018). The high-resolution AGCM simulations have also simulated the mean thermodynamic

Table 1
Details of the CESM1.2.2 and CAM5 Model Experiments

Model	Experiment	Duration	Forcing
CESM1.2.2 (fully coupled)	Control (CTRL)	350 years	Pre-industrial forcing
CESM1.2.2 (fully coupled)	Sea ice melt experiment (SIME)	50 years (branched off from 300th year of CTRL experiment)	Same as CTRL. In addition, we reduced the albedo of sea ice
CAM5	Control (CTRL-CAM5)	Four annual cycle runs of 4 years and another four annual cycle runs of 2 years (total of 24 annual cycles)	Year 2000 forcing for GHG, ozone, orbit, etc. Annual cycles of SST and sea ice concentration (SIC) from the CTRL simulation of fully coupled CESM CTRL run. The SST and SIC forcing data are created by computing monthly climatology from the last 10 years (year 341–350) of the fully coupled run
CAM5	Sea Ice Melt Experiment (SIME-CAM5)	Four annual cycle runs of 4 years and another four annual cycle runs of 2 years (total of 24 annual cycles)	Same as CTRL-CAM5 except that the SST and SIC annual cycles are created from the last 10 years of fully coupled SIME experiment

structure of ISM correctly (Sabin & Pauluis, 2020). The effect of global sea ice melt on ISMs mean and synoptic scale features is not understood. The synoptic scale vortices embedded in the monsoon circulation, known as LPS, contribute more than half of the total precipitation over continental India (Hunt et al., 2016; Praveen et al., 2015). Here, we investigate the response of monsoon LPS to the global sea ice melt using a series of coarse-resolution coupled and high-resolution uncoupled climate model simulations.

2. Data and Methods

We performed a control experiment (CTRL) by running the Community Earth System Model (CESM) version 1.2.2 (Hurrell et al., 2013) in a fully coupled configuration, with preindustrial (B1850_CAM5) forcing, for 350 years. The atmosphere and land are configured with a $0.9^\circ \times 1.25^\circ$ horizontal resolution, while the ocean and sea ice share a variable resolution $gx1v6$ displaced pole grid. In another experiment, the CESM model is restarted from the 300th year of the CTRL experiment and run for 50 years. In this experiment, we decreased the albedo of bare and ponded sea ice and snow cover on ice over the Arctic and Antarctic Oceans in the sea ice component of CESM. Specifically, we changed the parameters R_{ice} and R_{pnd} from 0 to -2 . Also, we reduced the single scattering albedo of snow by 10% for all spectral bands. These settings are similar to Liu and Fedorov (2019) where they found that the chosen values replicated the recently observed sea ice loss. We designate this simulation as a sea ice melt experiment (SIME). The SIC from phase five of the coupled model inter-comparison project (CMIP5; Taylor et al. (2012)) historical (1981–2000 period) and future projection (2081–2100 period) under the RCP8.5 scenario of CESM model have been used to compare with the CTRL and SIME simulations. It may be noted that our experiment design is different from that of the Polar Amplification Model Intercomparison Project (PAMIP) in which the models are nudged to the SST and SIC from the CMIP5 historical and future warming simulations (Smith et al., 2019). The 1-year time slice experiments of PAMIP may not be suitable for understanding the effects of SIC changes on low latitude climate, as the response through ocean dynamics can take several years to reach the tropics.

The current generation coupled models do not adequately resolve TCs and monsoon LPS when configured with a coarse horizontal resolution. We have designed a set of high-resolution AGCM simulations using the community atmospheric model (CAM5) to save computational resources. The CAM5 model is run at a 50 km horizontal resolution and forced with the annual cycles of SST and SIC from the CTRL and SIME simulations. We designate these experiments as CTRL-CAM5 and SIME-CAM5, respectively, to distinguish them from the coupled model experiments. The annual cycles of the monthly climatology of SST and SIC are constructed using the last 10 years of CTRL and SIME simulations. The other forcings of CAM5 are fixed at the year 2000 conditions for both experiments (Table 1). An ensemble of eight runs of CAM5 has been done by slightly perturbing the initial surface temperature for both experiments (Table 2). Four realizations are run for 4 years, and the remaining four realizations for 2 years. The first 5 months of the simulations are discarded for spin-up. Sandeep et al. (2018) performed similar high-resolution AGCM experiments forced with SST and SIC annual cycles from coupled

Table 2
Details of CAM5 CTRL and SIME Ensembles

Realizations	CTRL	SIME
PERT1	4 Years	4 Years
PERT2	4 Years	4 Years
PERT3	4 Years	4 Years
PERT4	4 Years	4 Years
PERT5	2 Years	2 Years
PERT6	2 Years	2 Years
PERT7	2 Years	2 Years
PERT8	2 Years	2 Years

Note. CAM5, community atmospheric model; CTRL, control; SIME, sea ice melt experiment.

models to investigate the changes in LPS activity in a warming scenario. In addition to the CAM5 experiments described in Table 1, we have run another set of CAM5 experiments for 4 years in which the preindustrial forcing parameters are used (F1850 forcing), while the SST and SIC boundary conditions are taken from the CTRL and SIME simulations of CESM1.2.2. This is done to examine the relative effects of preindustrial and current radiative forcing on the CAM5 model's response to the polar sea ice melt and associated SST changes.

The horizontal translation of monsoon LPS was explained by the vorticity advection mechanism (Boos et al., 2015). We have computed the absolute vorticity advection as $\mathbf{V} \cdot \nabla \eta$ where \mathbf{V} is the horizontal wind vector, and η is the absolute vorticity. The absolute vorticity advection is computed over 500–200 hPa.

We tracked the trajectories of LPS in the CAM5 simulations using Praveen et al. (2015) tracking algorithm. This algorithm detects and tracks LPS from gridded daily sea level pressure (SLP) data by identifying closed isobars at every 1 hPa interval. This algorithm also classifies the LPS according to their

intensity category based on the pressure depth (Δ SLP). The categorization of monsoon LPS over the Indian region is shown in Table 3.

3. Results and Discussion

The annual climatology of SIC over the Arctic simulated by the CTRL experiment is shown in Figure 1a. The northern hemispheric SIC in SIME run declined substantially as compared to CTRL (Figure 1b). The difference plot of SIC between SIME and CTRL shown in Figure 1c reveals that there is about a 50% decline in annual mean SIC over the Arctic in the SIME simulation, which is in line with the estimates of Liu and Fedorov (2019). The southern hemispheric SIC climatology simulated by the CTRL run is shown in Figure 1d. The annual mean Antarctic SIC is found to have declined by about 43% in the SIME experiment (Figures 1e and 1f). The annual cycles of monthly mean SIC over the Arctic and Antarctic in the CTRL and SIME experiments were computed and compared with the CMIP5 historical and RCP8.5 simulations of CESM (Figures 2a and 2b). The summer monsoon is sensitive to the SST of the tropical Indian and Pacific Oceans (Webster et al., 1998). The mean boreal summer SST response to the polar sea ice melt shows warming over all the ocean basins, with stronger warming over the tropical oceans (Figure 3).

The ensemble mean track density of LPS in CTRL runs of CAM5 shows a maximum in the LPS genesis over the head Bay of Bengal and adjoining continental India (Figure 4a). Further, the climatological LPS track density pattern in the CTRL-CAM5 ensemble has a close match with the earlier high-resolution AGCM simulations (Hurley & Boos, 2015; Krishnamurthy & Ajayamohan, 2010; Sandeep et al., 2018; Thomas et al., 2021). The LPS track density shows about 23% weakening in the SIME-CAM5 ensemble in comparison to the CTRL-CAM5 runs (Figure 4b). The difference plot between the SIME-CAM5 and CTRL-CAM5 shows a north-south dipole-like structure in the track density changes, with a strong weakening over the south and a strengthening over the north (Figure 4c). The area over which the track density weakens is more than double the area over which it strengthens. This indicates an overall weakening and a northward shift in LPS activity in SIME-CAM5 experiments. It is interesting to note that the pattern of changes in LPS track density is a close match with that reported by Sandeep et al. (2018) in their future warming projections. This suggests that the response of monsoon synoptic activity to the polar sea ice melt is similar to its response to increased radiative forcing.

The declined LPS activity in SIME-CAM5 simulations can be attributed to a decrease in the intensity of the storms or a decrease in the storm genesis frequency, or a combination of the two. The distribution of Δ SLP of LPS indicates the intensity of the storms during their life cycle (Figure 4d). The distribution of June–September (JJAS) mean LPS counts in each intensity

Table 3
Categorization of Monsoon LPS Based on Pressure Depth (Δ SLP)

Δ SLP (hPa)	LPS category
≤ 2	Low
> 2 and ≤ 4	Depression
> 4 and ≤ 10	Deep depression
> 10 and ≤ 16	Cyclonic storm
> 16	Severe cyclonic storm

Note. LPS, low-pressure systems; SLP, sea level pressure.

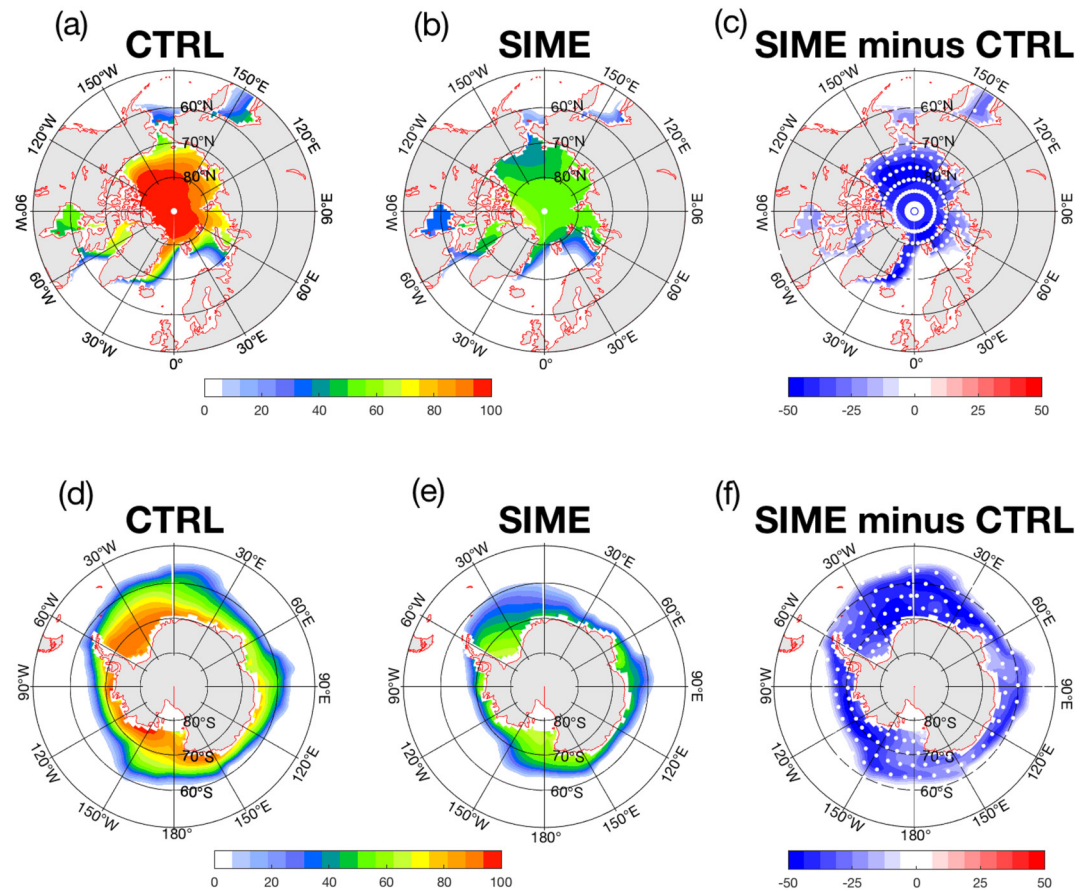


Figure 1. Annual mean climatology of sea ice concentration (SIC) (%) over the Arctic in (a) control (CTRL), (b) sea ice melt experiment (SIME) experiments, and (c) the difference in annual mean climatology of SIC over the Arctic between SIME and CTRL. (d–f) Same as (a–c), except for the Antarctic SIC. The climatology is constructed using the last 10 years of CTRL and SIME runs. Stippling in (c and f) denote the statistically significant ($p < 0.05$) difference between SIME and CTRL SIC over the Arctic and Antarctic, as revealed by a bootstrapping method.

category shows that the CTRL-CAM5 ensembles simulated a higher number of depressions followed by deep depressions and lows. The LPSs in the cyclonic storms and severe cyclonic storms categories are negligible in both the experiments (Figure 4e). The SIME-CAM5 shows a decrease in lows and depressions while the deep depressions remain the same as in the CTRL-CAM5 ensemble. This suggests that the weakening in LPS activity in response to polar sea ice melt is contributed by a decrease in the low-intensity systems. Overall, the LPS numbers in the CAM5-SIME ensemble decreased by about 22%. The CAM5 simulations performed with F1850 forcing parameters also show a weakening of monsoon synoptic activity in response to the polar sea ice melt (Figure S1 in Supporting Information S1). This suggests that the effects of SIC and SST changes may be driving the model response compared to the changes in the background radiative forcing. As a caveat, it is to be noted that we have performed only one realization of the CAM5 experiments with F1850 forcing and hence drawing a broader conclusion may not be appropriate.

Ditchek et al. (2016) found a relationship between the monthly mean fields of the monsoon and the monthly LPS genesis. A weakening in the mean low-level circulation and the associated vorticity in a warming climate was attributed to a significant decrease in the monsoon LPS activity simulated by an AGCM (Sandeep et al., 2018). The ensemble mean JJAS mean wind vectors and the absolute vorticity at 850 hPa resemble the typical ISM low-level flow pattern (Figure 5a). The maximum low-level vorticity is seen over the monsoon trough region, extending from northwest India to the head Bay of Bengal. The head Bay of Bengal is the core genesis region of monsoon LPS (Sikka, 1977). The wind vectors and absolute vorticity climatology from SIME-CAM5 simulations also show a similar pattern as in the CTRL-CAM5 runs (Figure 5b). To understand the difference between

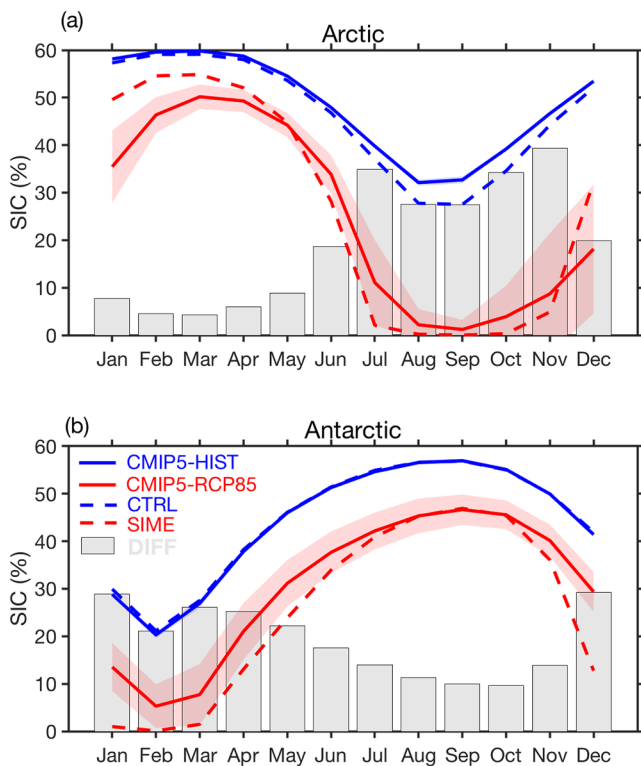


Figure 2. Seasonal cycle of sea ice concentration (SIC) over the (a) Arctic and (b) Antarctic from the control (CTRL), sea ice melt experiment (SIME), historical, and RCP8.5 simulations. The historical (RCP8.5) simulations of CESM1.1 for 1981–2000 (2081–2100) period are considered. The bars show the difference in SIC between CTRL and SIME experiments.

the two experiments, the difference in the wind vectors and absolute vorticity climatology between SIME-CAM5 and CTRL-CAM5 is computed (Figure 5c). The difference plot shows a north-south pattern identical to that of LPS track density, with a widespread weakening in the low-level circulation and absolute vorticity over the Bay of Bengal and the Arabian Sea and a moderate strengthening over the land region north of the head Bay of Bengal. The strengthening of the circulation in the north may be limited by the orography. These results suggest that the ISM circulation would undergo an overall weakening and northward shift in response to the melting of the Arctic and Antarctic sea ice. The changes in ISM low-level circulation and absolute vorticity explain the changes in the LPS activity in SIME-CAM5 experiments. In the CAM5 simulations using F1850 forcing, a weakening of the low-level monsoon flow can be seen in response to the polar sea ice melt, although the pattern of circulation change is slightly different (Figure S2 in Supporting Information S1).

The low-level circulation of the ISM was found to be weakening and shifting poleward in a warming climate (Sandeep & Ajayamohan, 2015). Recent studies indicate that the polar sea ice melt in climate model simulations produces climate system response patterns reminiscent of global warming induced by GHG emissions (England et al., 2020; Liu & Fedorov, 2019). It was also suggested that the combined Arctic and Antarctic sea ice melt might account for about a third of tropical warming through the response of ocean dynamics (England et al., 2020). The pattern of tropical SST warming in the SIME run is in line with the arguments of England et al. (2020) (Figure 3). A closer examination of the SST warming patterns reveals that the southern Indian Ocean warms stronger than the northern Indian Ocean in SIME simulations using the coupled model. This can lead to a weakening of the meridional SST gradient that in turn results in the weakening of ISM circulation. The relative contributions of Arctic and Antarctic sea ice melt to the response of ISM need to be examined by conducting additional experiments. We may

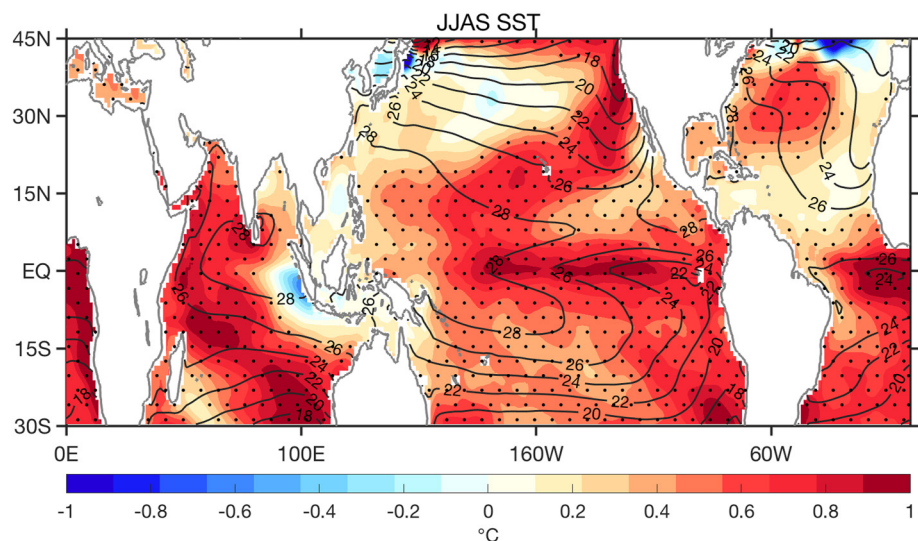


Figure 3. June–September mean climatology of sea surface temperature from control (CTRL) simulation (contours; unit: °C) and the difference between sea ice melt experiment (SIME) and CTRL simulations (shading). Stippling denotes the statistically significant ($p < 0.05$) difference between SIME and CTRL, as revealed by a bootstrapping method. The calculations are based on the last 10 years (year 341–350) of coupled model simulations.

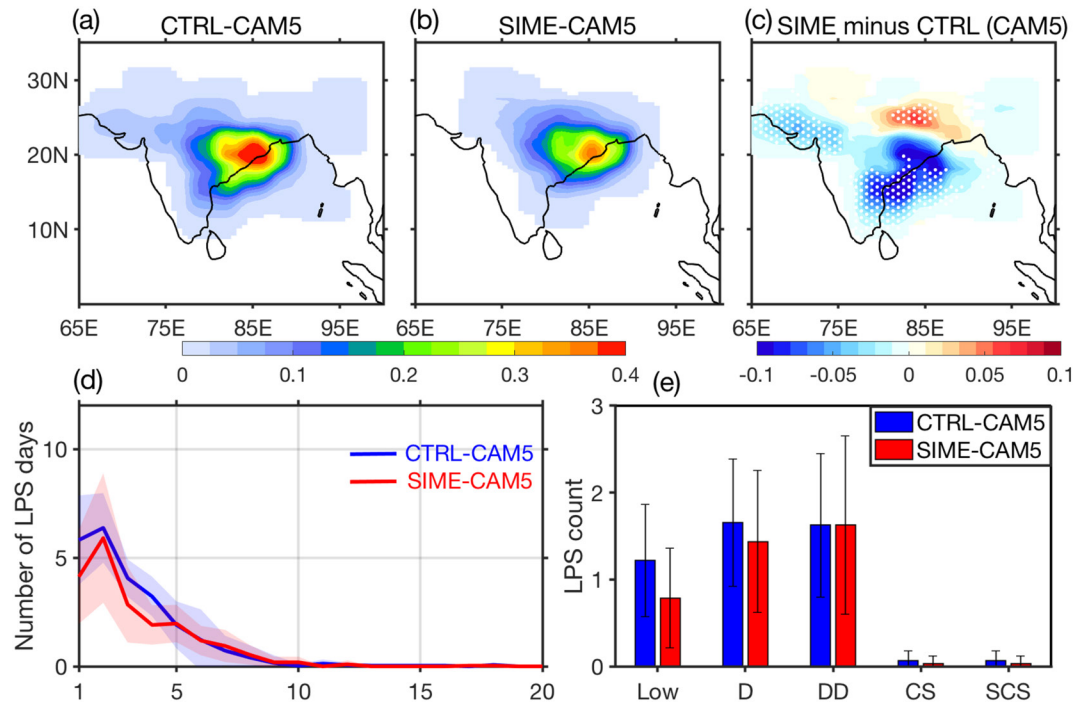


Figure 4. June–September (JJAS) mean, ensemble mean low-pressure systems (LPS) track density (unit: number of LPS per grid per season) for (a) CTRL-CAM5 and (b) SIME-CAM5 simulations; (c) ensemble mean difference between SIME-CAM5 and CTRL-CAM5 track density, (d) JJAS mean distributions of LPS days as a function of pressure depth (Δ SLP) of LPS, and (e) category-wise distribution of JJAS mean LPS counts in model simulations. Stippling in (c) denotes the statistically significant ($p < 0.05$) difference between SIME-CAM5 and CTRL-CAM5 LPS track density, as revealed by a bootstrapping method. The blue (red) shading in (d) shows the ensemble spread in CTRL-CAM5 and (SIME-CAM5) experiments. The error bars in (e) also show ensemble spread (± 1 std) in CTRL-CAM5 and SIME-CAM5 runs.

speculate that the Arctic sea ice melt is the major contributor to the changes in the northern hemispheric summer, based on the annual cycle of SIC in the SIME simulation.

Recent evidence suggests an equatorward shift in the ITCZ in response to the Arctic sea ice melt (Deser et al., 2015; Liu & Fedorov, 2019). Such a shift in ITCZ can result in a weakening of the cyclogenesis (Ballinger et al., 2015; Merlis et al., 2013). We examine the changes in the regional ITCZ over the Indian monsoon region

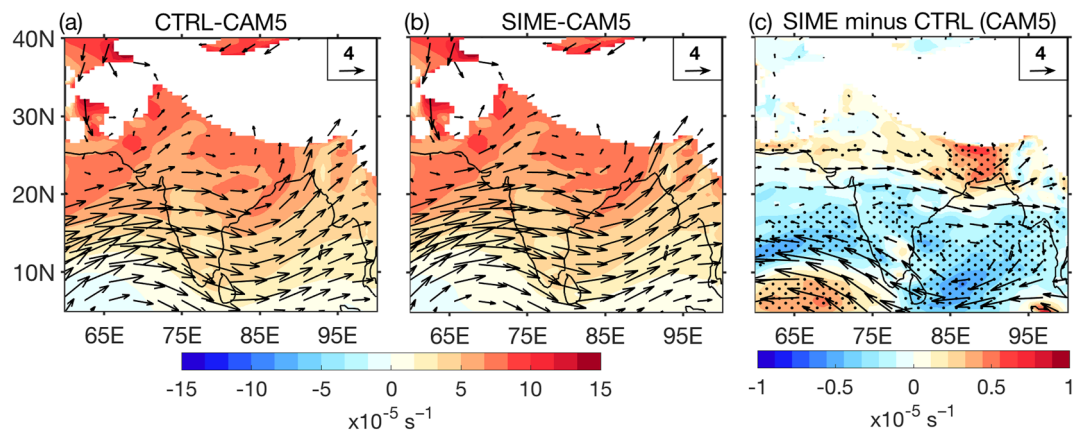


Figure 5. June–September mean, ensemble mean wind vectors and absolute vorticity at 850 hPa for (a) CTRL-CAM5 and (b) SIME-CAM5 simulations, and (c) ensemble mean SIME-CAM5 minus CTRL-CAM5 wind vectors and absolute vorticity at 850 hPa. Stippling in (c) denotes the statistically significant (at 95% confidence level) difference between SIME-CAM5 and CTRL-CAM5 absolute vorticity, as revealed by a bootstrapping method.

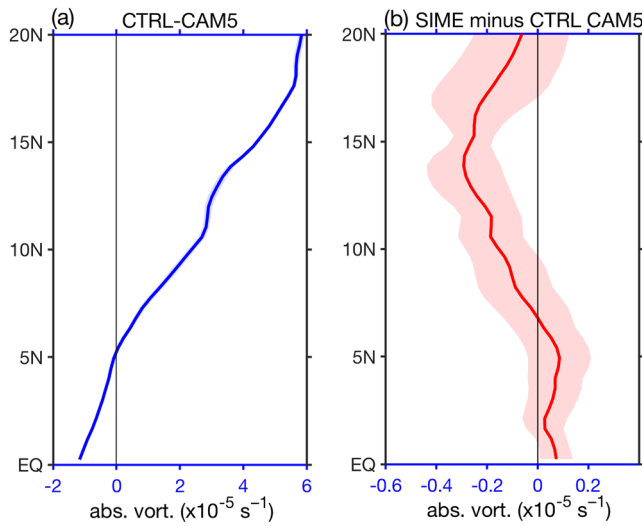


Figure 6. July and August mean zonal mean (50°E–100°E) absolute vorticity at 850 hPa from (a) CTRL-CAM5 simulations and (b) difference in July and August mean absolute vorticity between SIME-CAM5 and CTRL-CAM5 simulations. The solid line shows the ensemble mean and the shading ensemble spread.

that may explain the decline in LPS activity. The ITCZ can be identified as the centroid of maximum precipitation or the latitude of low-level zero absolute vorticity (Liu & Fedorov, 2019; Tomas & Webster, 1997). The zonal mean ensemble mean July and August absolute vorticity at 850 hPa from the CTRL-CAM5 experiments show a change of sign at around 6°N and a maximum around 20°N (Figure 6a). We chose July and August as it is the peak LPS genesis period. The ensemble mean difference in the July and August zonal mean absolute vorticity shows a weakening north of about 7°N and a relative strengthening in the equatorward region (Figure 6b). This indicates a decrease in the convergence over the core LPS genesis region and an equatorward shift in the ITCZ.

The mid-tropospheric relative humidity and wind shear are also critical parameters that can influence the genesis of cyclonic storms (Gray, 1998; Sikka, 1977). Hence, we examined the relative humidity at 500 hPa in the CTRL-CAM5 and SIME-CAM5 ensembles for the JJAS season (Figures 7a and 7b). The mid-tropospheric relative humidity over the Bay of Bengal in both experiments is found to be greater than 70%. The ensemble mean difference in the 500 hPa relative humidity between SIME-CAM5 and CTRL-CAM5 ensembles reveals a strong decrease in the mid-tropospheric moistening over the southern Arabian Sea and the Bay of Bengal in sea ice melt experiments (Figure 7c). However, the changes in mid-tropospheric relative humidity over the core LPS genesis region are not significant, suggesting that it may not contribute to the weakening of LPS activity in CAM5-SIME experiments.

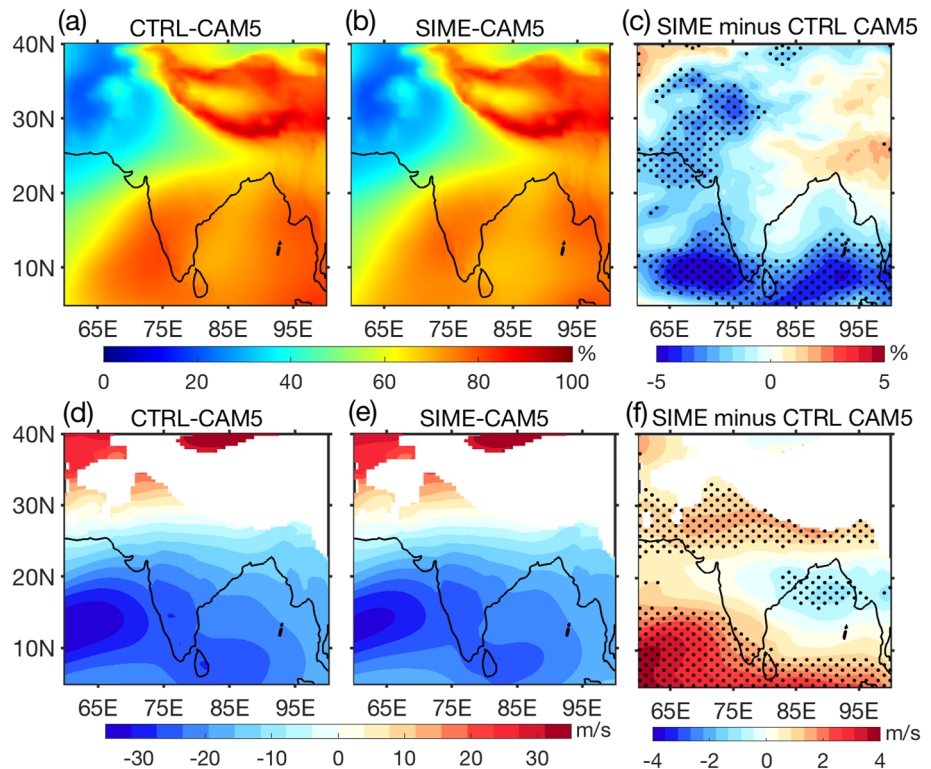


Figure 7. June–September mean, ensemble mean relative humidity at 500 hPa and vertical wind shear (U200 minus U850) for (a) CTRL-CAM5 and (b) SIME-CAM5 simulations, and (c) ensemble mean SIME-CAM5 minus CTRL-CAM5 relative humidity at 500 hPa. (d–f) Same as (a–c), except for the vertical wind shear (U200 minus U850). Stippling in (c and f) denotes the statistically significant ($p < 0.05$) difference between SIME-CAM5 and CTRL-CAM5, as revealed by a bootstrapping method.

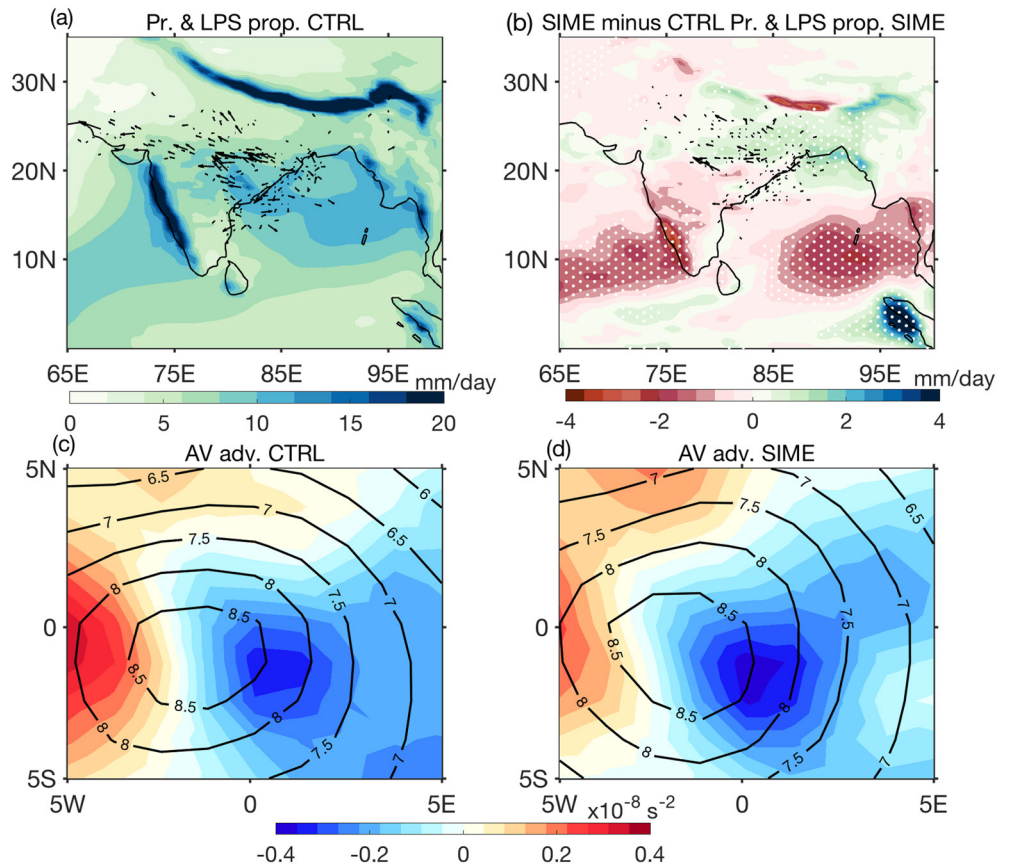


Figure 8. Top panel: Composites of (a) ensemble mean June–September mean precipitation (shading) and low-pressure systems (LPS) propagation vectors from CTRL-CAM5 and (b) difference in precipitation (shading) between SIME-CAM5 and CTRL-CAM5, and LPS propagation vectors in SIME-CAM5. Stippling shows a statistically significant (at 95% confidence level) change in precipitation as revealed by a *t*-test. Bottom panel: LPS-centered composites of 500–250 hPa averaged absolute vorticity (contours; units: $\times 10^{-5} \text{ s}^{-1}$) and absolute vorticity advection (shading; units: $\times 10^{-8} \text{ s}^{-2}$) for (c) CTRL-CAM5 and (d) SIME-CAM5 simulations. The coordinates in (c) and (d) are relative to the LPS center.

The vertical wind shear in CTRL-CAM5 and SIME-CAM5 over the Bay of Bengal is in the range from -10 to -20 m s^{-1} (Figures 7d and 7e). The ensemble mean difference in the vertical wind shear between SIME-CAM5 and CTRL-CAM5 reveals a significant strengthening of vertical shear over the head Bay of Bengal, which is the core LPS genesis region (Figure 7f). This suggests that a stronger vertical shear also has played a role in the weakening of LPS activity in SIME-CAM5 experiments.

The propagation of LPS to the deep interior parts of the Indian landmass plays a crucial role in the distribution of precipitation during the summer monsoon season. The ensemble mean translation vectors of LPS from the CTRL-CAM5 simulations show a north-westward propagation (Figure 8a) that is closely comparable with the observed horizontal advection of LPS (Hurley & Boos, 2015; Krishnamurthy & Ajayamohan, 2010; Srujan et al., 2021). The LPS propagation in the SIME-CAM5 ensemble is weak and not penetrating to northwestern India (Figure 8b). It is found that the frequency of an LPS crossing 20°N and 77°E is reduced by about 56% in the CAM5-SIME ensemble. One of the suggested mechanisms of the LPS propagation is the vorticity advection. The storm-centered composite of 500–250 hPa averaged absolute vorticity shows a maximum in the southwest quadrant of the storm in the CTRL-CAM5 ensemble (Figure 8c) as observed (Hurley & Boos, 2015; Sikka, 1977). The advection of absolute vorticity shows a westward propagation that explains to a considerable extent the simulated LPS propagation. In the SIME-CAM5 ensemble, the absolute vorticity and the advection of the absolute vorticity associated with the simulated LPS weaken (Figure 8d). This explains the weaker LPS propagation in the SIME-CAM5 simulations.

The seasonal mean precipitation climatology in the CTRL-CAM5 ensemble shows a band of nonorographic precipitation maxima aligned with the LPS propagation vectors (Figure 8a). A widespread weakening of ISM precipitation can be seen in the SIME-CAM5 ensemble, a part of which might be contributed by the weaker LPS activity (Figure 8b). An increase in rainfall over eastern and northeastern India is seen in the CAM5-SIME simulations. Earlier, Ajayamohan et al. (2010) reported an increasing trend in the extreme precipitation over continental India due to an increase in the land-based weak LPS. The increase in the LPS track density seen in the SIME-CAM5 experiments might be the reason for increased precipitation over eastern India. Also, an increased convergence over the land in the SIME-CAM5 ensemble (Figure 5c) can contribute to increased rainfall over eastern and northeastern India.

4. Conclusions

The oceans over the Arctic and Antarctic regions are projected to have ice-free summers toward the end of the 21st century in simulations of high emission scenarios. The global sea ice melting is shown to affect the tropical climate, primarily through ocean dynamics. However, the effect of sea ice melt on major tropical climate systems such as the ISM was not understood. We have performed a suite of coupled and uncoupled climate model simulations to understand the impact of global sea ice melt on the ISM synoptic activity. Our results show that the ISM circulation would weaken significantly due to the global sea ice melt. Further, the monsoon LPS, responsible for more than half of the continental Indian rainfall, weakened and underwent a northward shift in the sea ice melt simulations. The changes in the low-level absolute vorticity and vertical shear over the Bay of Bengal explained the changes in LPS activity in response to polar sea ice melt. Overall, the changes in ISM circulation and LPS activity in response to polar sea ice melt were similar to the changes seen in future warming projections under strong emission scenarios. This indicates that the polar sea ice melt might amplify the effects of radiative forcing due to enhanced GHG emissions. Our results clearly suggest that the polar sea ice melt can create a climate system response in the deep tropics, with substantial societal implications. In the present study, we have examined a scenario in which the sea ice over both hemispheres would melt. However, in the backdrop of the present results, it is important to investigate the relative contributions by the Arctic and Antarctic sea ice melt separately.

Data Availability Statement

The CESM-CAM5 model simulations and LPS tracks data (Chandra et al., 2022) can be accessed from <https://doi.org/10.5281/zenodo.6631947>.

Acknowledgments

S. Sandeep acknowledges the financial support given by the ESSO-National Centre for Polar and Ocean Research, Ministry of Earth Sciences, Government of India under the PACER outreach programme initiative (NCPOR/2019/PACER-POP/OS-04). The coupled and uncoupled simulations of CESM are performed on the High Performance Computing resources of IIT Delhi.

References

- Ajayamohan, R. S., Merryfield, W. J., & Kharin, V. V. (2010). Increasing trend of synoptic activity and its relationship with extreme rain events over central India. *Journal of Climate*, 23(4), 1004–1013. <https://doi.org/10.1175/2009JCLI2918.1>
- Ballinger, A. P., Merlis, T. M., Held, I. M., & Zhao, M. (2015). The sensitivity of tropical cyclone activity to off-equatorial thermal forcing in aquaplanet simulations. *Journal of the Atmospheric Sciences*, 72(6), 2286–2302. <https://doi.org/10.1175/JAS-D-14-0284.1>
- Barnes, E. A., Dunn-Sigouin, E., Masato, G., & Woollings, T. (2014). Exploring recent trends in Northern Hemisphere blocking. *Geophysical Research Letters*, 41(2), 638–644. <https://doi.org/10.1002/2013GL058745>
- Berry, G., & Reeder, M. J. (2014). Objective identification of the intertropical convergence zone: Climatology and trends from the era-interim. *Journal of Climate*, 27(5), 1894–1909. <https://doi.org/10.1175/JCLI-D-13-00339.1>
- Boos, W. R., Hurley, J. V., & Murthy, V. S. (2015). Adiabatic westward drift of Indian monsoon depressions. *Quarterly Journal of the Royal Meteorological Society*, 141(689), 1035–1048. <https://doi.org/10.1002/qj.2454>
- Budikova, D. (2009). Role of Arctic sea ice in global atmospheric circulation: A review. *Global and Planetary Change*, 68(3), 149–163. <https://doi.org/10.1016/j.gloplacha.2009.04.001>
- Buermann, W., Lintner, B., & Bonfils, C. (2005). A wintertime Arctic oscillation signature on early-season Indian Ocean monsoon intensity. *Journal of Climate*, 18(13), 2247–2269. <https://doi.org/10.1175/JCLI3377.1>
- Chandra, V., Sandeep, S., Suhas, E., & Subramanian, A. C. (2022). Dataset for "Weakening of Indian summer monsoon synoptic activity in response to polar sea ice melt induced by albedo reduction in a climate model." *Zenodo*. <https://doi.org/10.5281/zenodo.6631947>
- Chatterjee, S., Ravichandran, M., Murukesh, N., Raj, R. P., & Johannessen, O. M. (2021). A possible relation between Arctic sea ice and late season Indian summer monsoon rainfall extremes. *npj Climate and Atmospheric Science*, 4(1), 36. <https://doi.org/10.1038/s41612-021-00191-w>
- Cohen, J., Screen, J., Furtado, J., Barlow, M., Whittleston, D., Coumou, D., et al. (2014). Recent Arctic amplification and extreme mid-latitude weather. *Nature Geoscience*, 7(9), 627–637. <https://doi.org/10.1038/ngeo2234>
- Cohen, J., Zhang, X., Francis, J., Jung, T., Kwok, R., Overland, J., et al. (2020). Divergent consensus on Arctic amplification influence on midlatitude severe winter weather. *Nature Climate Change*, 10(1), 20–29. <https://doi.org/10.1038/s41558-019-0662-y>
- Deng, K., Yang, S., Ting, M., Hu, C., & Lu, M. (2018). Variations of the mid-Pacific trough and their relations to the Asian–Pacific–North American climate: Roles of tropical sea surface temperature and Arctic sea ice. *Journal of Climate*, 31(6), 2233–2252. <https://doi.org/10.1175/JCLI-D-17-0064.1>

- Deser, C., Tomas, R., Alexander, M., & Lawrence, D. (2010). The seasonal atmospheric response to projected Arctic sea ice loss in the late twenty-first century. *Journal of Climate*, 23(2), 333–351. <https://doi.org/10.1175/2009JCLI3053.1>
- Deser, C., Tomas, R. A., & Sun, L. (2015). The role of ocean–atmosphere coupling in the zonal-mean atmospheric response to Arctic sea ice loss. *Journal of Climate*, 28(6), 2168–2186. <https://doi.org/10.1175/JCLI-D-14-00325.1>
- Ditchek, S. D., Boos, W. R., Camargo, S. J., & Tippett, M. K. (2016). A genesis index for monsoon disturbances. *Journal of Climate*, 29(14), 5189–5203. <https://doi.org/10.1175/JCLI-D-15-0704.1>
- Dong, W., Ming, Y., & Ramaswamy, V. (2020). Projected changes in South Asian monsoon low pressure systems. *Journal of Climate*, 33(17), 7275–7287. <https://doi.org/10.1175/JCLI-D-20-0168.1>
- England, M., Polvani, L., Sun, L., & Deser, C. (2020). Tropical climate responses to projected Arctic and Antarctic sea-ice loss. *Nature Geoscience*, 13(4), 275–281. <https://doi.org/10.1038/s41561-020-0546-9>
- Francis, J. A., Chan, W., Leathers, D. J., Miller, J. R., & Veron, D. E. (2009). Winter Northern Hemisphere weather patterns remember summer Arctic sea-ice extent. *Geophysical Research Letters*, 36(7), L07503. <https://doi.org/10.1029/2009GL037274>
- Francis, J. A., & Vavrus, S. J. (2012). Evidence linking Arctic amplification to extreme weather in mid-latitudes. *Geophysical Research Letters*, 39(6), L06801. <https://doi.org/10.1029/2012GL051000>
- Gray, W. M. (1998). The formation of tropical cyclones. *Meteorology and Atmospheric Physics*, 67(1–4), 37–69. <https://doi.org/10.1007/BF01277501>
- Guo, D., Gao, Y., Bethke, I., Gong, D., Johannessen, O. M., & Wang, H. (2014). Mechanism on how the spring Arctic sea ice impacts the East Asian summer monsoon. *Theoretical and Applied Climatology*, 115(1–2), 107–119. <https://doi.org/10.1007/s00704-013-0872-6>
- Hunt, K. M. R., Turner, A. G., & Parker, D. E. (2016). The spatiotemporal structure of precipitation in Indian monsoon depressions. *Quarterly Journal of the Royal Meteorological Society*, 142(701), 3195–3210. <https://doi.org/10.1002/qj.2901>
- Hurley, J. V., & Boos, W. R. (2015). A global climatology of monsoon low-pressure systems. *Quarterly Journal of the Royal Meteorological Society*, 141(689), 1049–1064. <https://doi.org/10.1002/qj.2447>
- Hurrell, J. W., Holland, M. M., Gent, P. R., Ghan, S., Kay, J. E., Kushner, P. J., et al. (2013). The community Earth system model: A framework for collaborative research. *Bulletin of the American Meteorological Society*, 94(9), 1339–1360. <https://doi.org/10.1175/BAMS-D-12-00121.1>
- Khandekar, M. (1991). Eurasian snow cover, Indian monsoon and El Niño/Southern Oscillation – A synthesis. *Atmosphere-Ocean*, 29(4), 636–647. <https://doi.org/10.1080/07055900.1991.9649422>
- Krishnamurthy, V., & Ajayamohan, R. S. (2010). Composite structure of monsoon low pressure systems and its relation to Indian rainfall. *Journal of Climate*, 23(16), 4285–4305. <https://doi.org/10.1175/2010JCLI2953.1>
- Krishnamurti, T. N., Krishnamurti, R., Das, S., Kumar, V., Jayakumar, A., & Simon, A. (2015). A pathway connecting the monsoonal heating to the rapid Arctic ice melt. *Journal of the Atmospheric Sciences*, 72(1), 5–34. <https://doi.org/10.1175/JAS-D-14-0004.1>
- Lindsay, R. W., & Zhang, J. (2005). The thinning of Arctic Sea ice, 1988–2003: Have we passed a tipping point? *Journal of Climate*, 18(22), 4879–4894. <https://doi.org/10.1175/JCLI3587.1>
- Liu, W., & Fedorov, A. V. (2019). Global impacts of Arctic Sea ice loss mediated by the Atlantic meridional overturning circulation. *Geophysical Research Letters*, 46(2), 944–952. <https://doi.org/10.1029/2018GL080602>
- Meera, M., Suhas, E., & Sandeep, S. (2019). Downstream and in situ: Two perspectives on the initiation of monsoon low-pressure systems over the Bay of Bengal. *Geophysical Research Letters*, 46(21), 12303–12310. <https://doi.org/10.1029/2019GL084555>
- Merlis, T. M., Zhao, M., & Held, I. M. (2013). The sensitivity of hurricane frequency to ITCZ changes and radiatively forced warming in aquaplanet simulations. *Geophysical Research Letters*, 40(15), 4109–4114. <https://doi.org/10.1002/grl.50680>
- Molinari, J., & Vollaro, D. (2013). What percentage of Western North Pacific tropical cyclones form within the monsoon trough? *Monthly Weather Review*, 141(2), 499–505. <https://doi.org/10.1175/MWR-D-12-00165.1>
- Murakami, H., Wang, B., & Kitoh, A. (2011). Future change of western north Pacific typhoons: Projections by a 20-km-mesh global atmospheric model. *Journal of Climate*, 24(4), 1154–1169. <https://doi.org/10.1175/2010JCLI3723.1>
- Nuncio, M., Chatterjee, S., Satheesan, K., Chenoli, S. N., & Subeesh, M. P. (2020). Temperature and precipitation during winter in nyÅlesund, svalbard and possible tropical linkages. *Tellus A: Dynamic Meteorology and Oceanography*, 72(1), 1–15. <https://doi.org/10.1080/16000870.2020.1746604>
- Overland, J. E., & Wang, M. (2013). When will the summer Arctic be nearly sea ice free? *Geophysical Research Letters*, 40(10), 2097–2101. <https://doi.org/10.1002/grl.50316>
- Parkinson, C. L. (2019). A 40-y record reveals gradual Antarctic sea ice increases followed by decreases at rates far exceeding the rates seen in the Arctic. *Proceedings of the National Academy of Sciences*, 116(29), 14414–14423. <https://doi.org/10.1073/pnas.1906556116>
- Pottapinjara, V., Girishkumar, M. S., Ravichandran, M., & Murtugudde, R. (2014). Influence of the Atlantic zonal mode on monsoon depressions in the Bay of Bengal during boreal summer. *Journal of Geophysical Research: Atmospheres*, 119, 6456–6469. <https://doi.org/10.1002/2014JD021494>
- Prabhu, A., Mahajan, P., & Khaladkar, R. (2012). Association of the Indian summer monsoon rainfall variability with the geophysical parameters over the Arctic region. *International Journal of Climatology*, 32(13), 2042–2050. <https://doi.org/10.1002/joc.2418>
- Prabhu, A., Mandke, S. K., Kripalani, R., & Pandithurai, G. (2021). Association between Antarctic sea ice, Pacific SST and the Indian summer monsoon: An observational study. *Polar Science*, 30, 100746. <https://doi.org/10.1016/j.polar.2021.100746>
- Praveen, V., Sandeep, S., & Ajayamohan, R. S. (2015). On the relationship between mean monsoon precipitation and low pressure systems in climate model simulations. *Journal of Climate*, 28(13), 5305–5324. <https://doi.org/10.1175/JCLI-D-14-00415.1>
- Rajeevan, M. (2002). Winter surface pressure anomalies over Eurasia and Indian summer monsoon. *Geophysical Research Letters*, 29(10), 1–4. <https://doi.org/10.1029/2001GL014363>
- Rastogi, D., Ashfaq, M., Leung, L. R., Ghosh, S., Saha, A., Hodges, K., & Evans, K. (2018). Characteristics of Bay of Bengal monsoon depressions in the 21st century. *Geophysical Research Letters*, 45(13), 6637–6645. <https://doi.org/10.1029/2018GL078756>
- Rinke, A., Maturilli, M., Graham, R. M., Matthes, H., Handorf, D., Cohen, L., et al. (2017). Extreme cyclone events in the Arctic: Wintertime variability and trends. *Environmental Research Letters*, 12(9), 094006. <https://doi.org/10.1088/1748-9326/aa7def>
- Roach, L. A., Dörr, J., Holmes, C. R., Massonnet, F., Blockley, E. W., Notz, D., et al. (2020). Antarctic sea ice area in CMIP6. *Geophysical Research Letters*, 47(9), e2019GL086729. <https://doi.org/10.1029/2019GL086729>
- Sabeerali, C. T., Ajayamohan, R. S., Bangalath, H. K., & Chen, N. (2019). Atlantic zonal mode: An emerging source of Indian summer monsoon variability in a warming world. *Geophysical Research Letters*, 46(8), 4460–4467. <https://doi.org/10.1029/2019GL082379>
- Sabeerali, C. T., Ajayamohan, R. S., & Praveen, V. (2021). Atlantic zonal mode-monsoon teleconnection in a warming scenario. *Climate Dynamics*, 58(5–6), 1829–1843. <https://doi.org/10.1007/s00382-021-05996-2>
- Sabin, T. P., Krishnan, R., Ghattas, J., Denvil, S., Dufresne, J.-L., Hourdin, F., & Pascal, T. (2013). High resolution simulation of the South Asian monsoon using a variable resolution global climate model. *Climate Dynamics*, 41(1), 173–194. <https://doi.org/10.1007/s00382-012-1658-8>

- Sabin, T. P., & Pauluis, O. M. (2020). The South Asian monsoon circulation in moist isentropic coordinates. *Journal of Climate*, *33*(12), 5253–5270. <https://doi.org/10.1175/JCLI-D-19-0637.1>
- Sandeep, S., & Ajayamohan, R. S. (2015). Poleward shift in Indian summer monsoon low level jetstream under global warming. *Climate Dynamics*, *45*(1–2), 337–351. <https://doi.org/10.1007/s00382-014-2261-y>
- Sandeep, S., Ajayamohan, R. S., Boos, W. R., Sabin, T. P., & Praveen, V. (2018). Decline and poleward shift in Indian summer monsoon synoptic activity in a warming climate. *Proceedings of the National Academy of Sciences*, *115*(11), 2681–2686. <https://doi.org/10.1073/pnas.1709031115>
- Screen, J. A., & Simmonds, I. (2010). Increasing fall-winter energy loss from the Arctic Ocean and its role in Arctic temperature amplification. *Geophysical Research Letters*, *37*(16). <https://doi.org/10.1029/2010GL044136>
- Serreze, M. C., & Barry, R. G. (2011). Processes and impacts of Arctic amplification: A research synthesis. *Global and Planetary Change*, *77*(1), 85–96. <https://doi.org/10.1016/j.gloplacha.2011.03.004>
- Sevellec, F., Fedorov, A., & Liu, W. (2017). Arctic sea-ice decline weakens the Atlantic meridional overturning circulation. *Nature Climate Change*, *7*(8), 604–610. <https://doi.org/10.1038/nclimate3353>
- Sikka, D. R. (1977). Some aspects of the life history, structure and movement of monsoon depressions. *Pure and Applied Geophysics*, *115*(5–6), 1501–1529. <https://doi.org/10.1007/BF00874421>
- Smeed, D. A., McCarthy, G. D., Cunningham, S. A., Frajka-Williams, E., Rayner, D., Johns, W. E., et al. (2014). Observed decline of the Atlantic meridional overturning circulation 2004–2012. *Ocean Science*, *10*(1), 29–38. <https://doi.org/10.5194/os-10-29-2014>
- Smith, D. M., Screen, J. A., Deser, C., Cohen, J., Fyfe, J. C., García-Serrano, J., et al. (2019). The polar amplification model intercomparison project (PAMIP) contribution to CMIP6: Investigating the causes and consequences of polar amplification. *Geoscientific Model Development*, *12*(3), 1139–1164. <https://doi.org/10.5194/gmd-12-1139-2019>
- Sørland, S. L., Sorteberg, A., Liu, C., & Rasmussen, R. (2016). Precipitation response of monsoon low-pressure systems to an idealized uniform temperature increase. *Journal of Geophysical Research: Atmospheres*, *121*, 6258–6272. <https://doi.org/10.1002/2015JD024658>
- Srujan, K. S. S. S., Sandeep, S., & Suhas, E. (2021). Downstream and in situ genesis of monsoon low-pressure systems in climate models. *Earth and Space Science*, *8*(9), e2021EA001741. <https://doi.org/10.1029/2021EA001741>
- Srujan, K. S. S. S., Sandeep, S., Suhas, E., & Kodamana, H. (2022). A dynamical linkage between Western North Pacific tropical cyclones and Indian monsoon low-pressure systems. *Geophysical Research Letters*, *49*(11), e2022GL098597. <https://doi.org/10.1029/2022GL098597>
- Taylor, K. E., Stouffer, R. J., & Meehl, G. A. (2012). An overview of CMIP5 and the experiment design. *Bulletin of the American Meteorological Society*, *93*(4), 485–498. <https://doi.org/10.1175/BAMS-D-11-00094.1>
- Thomas, T., Bala, G., & Srinivas, V. (2021). Characteristics of the monsoon low pressure systems in the Indian subcontinent and the associated extreme precipitation events. *Climate Dynamics*, *56*(5–6), 1859–1878. <https://doi.org/10.1007/s00382-020-05562-2>
- Tomas, R. A., Deser, C., & Sun, L. (2016). The role of ocean heat transport in the global climate response to projected Arctic sea ice loss. *Journal of Climate*, *29*(19), 6841–6859. <https://doi.org/10.1175/JCLI-D-15-0651.1>
- Tomas, R. A., & Webster, P. J. (1997). The role of inertial instability in determining the location and strength of near-equatorial convection. *Quarterly Journal of the Royal Meteorological Society*, *123*(542), 1445–1482. <https://doi.org/10.1002/qj.49712354202>
- Wallace, J. M., Held, I. M., Thompson, D. W. J., Trenberth, K. E., & Walsh, J. E. (2014). Global warming and winter weather. *Science*, *343*(6172), 729–730. <https://doi.org/10.1126/science.343.6172.729>
- Webster, P. J., Magaña, V. O., Palmer, T. N., Shukla, J., Tomas, R. A., Yanai, M., & Yasunari, T. (1998). Monsoons: Processes, predictability, and the prospects for prediction. *Journal of Geophysical Research*, *103*(C7), 14451–14510. <https://doi.org/10.1029/97JC02719>